A Parametric Study of Inertia Friction Welding for Low Alloy Steel Pipes

Speed of rotation and moment of inertia of the flywheel system are the controlling factors affecting weld microstructures

BY M. D. TUMULURU

ABSTRACT. The effect of welding variables on the resultant microstructures was studied in the inertia friction welding of low alloy steel pipes. The weld microstructures were studied in the as-welded condition. Notched tensile and impact tests were conducted on selected welds in the quenched and tempered condition.

The study indicated that the weld microstructures are controlled by the speed of rotation and the moment of inertia of the flywheel system, while the axial pressure did not have any significant effect. The welds tested exhibited poor toughness, probably due to the reorientation of the grains at the weld interface. No significant bulk compositional changes were detected in the surface layers of the weld interfaces compared to the unaffected base materials.

Introduction

The inertia friction welding process is one of the methods currently being utilized in this country and abroad for the fabrication of drill pipes used in the oil drilling industry. Each drill pipe consists of a central tubular section called the pipe that is welded to couplings called tool joints. The male coupling, called the pin, contains external threads, while the female coupling, called the box, has internal threads. Both the tool joints are generally made of quenched-and-tempered AISI 4137-H steel and can be welded to the pipe using inertia friction welding.

The inertia friction welding process, also known commercially as flywheel friction welding, is a solid state welding technique wherein the energy required to form the bond between the pieces to be joined is stored in a flywheel (Ref. 1). In the actual process, one of the parts to be joined is clamped in a chuck mounted on to a rotating spindle and rotated to a predetermined speed. Then, the rotating power is cut off, and the stationary part is brought into contact with the moving part under an applied axial pressure. The friction between the parts not only brings the moving part to a halt but also generates sufficient heat to achieve the weld between the pieces.

Due to the application of the axial pressure, the hot metal at the periphery of the parts to be joined is squeezed out plastically. The metal that is pushed out plastically at the outer and inner diameters is termed the "flash." Since part of the metal from both the pieces to be joined is removed as flash, the total length of the pieces joined is reduced after welding is completed. This reduction in the total length of the parts after they are welded is termed as "upset" (Ref. 2).

Inertia friction welding is an attractive process for the welding of drill pipes because of the short time required for the operation. Typically, pipes with outer diameters up to 130 mm (5.12 in.) and wall thicknesses of 20 mm (0.79 in.) can be welded in less than 15 seconds (s).

Much of the earlier published work on inertia friction welding had been concentrated on understanding the mechanism of bonding, the thermal behavior of the process, and studying the feasibility of the process for the joining of dissimilar metals and alloys (Refs. 3-9). Very little research has been reported on the metallurgical aspects of the inertia friction welding process. The purpose of the present investigation was to study the effects of the welding variables on the resultant weld shapes and microstructures in the inertia friction welding of low alloy steel pipes.

Materials and Experimental Procedure

The test welds were made between dissimilar steels—steel A (AISI 4137-H) and steel B. Steel B corresponds to API grade E pipe (per API specification 5A). The only API Specification 5A chemistry requirements for grade E pipe are that the phosphorus and sulfur contents be limited to 0.040% and 0.060% max each, respectively.

The end couplings made of steel A were used in the quenched-and-tempered condition, whereas the pipes made of steel B were normalized and tempered. Typical compositions of steel A and steel B used in making the test welds are listed in Table 1.

The wall thickness and the outside diameter at the mating faces of the pipes chosen for the study were 17 and 115 mm (0.67 and 4.52 in.), respectively. The mating faces of the end couplings and the pipe were machined flat in a lathe to avoid any mismatch. The surface rough-

Table 1—Chemical Compositions of the Steels Used in the Study, %

Element	Steel A (coupling material)	Steel B (pipe)
C	0.41	0.43
Mn	0.86	1.72
Si	0.24	0.22
Ni	0.13	<0.005
Mo	0.20	0.15
Cu	0.11	0.02
Cr	0.90	0.03
S	0.010	0.011
P	0.010	0.010

M. D. TUMULURU is Research Metallurgist, Spang & Company, Butler, Pennsylvania.

Table 2—Test Welding Variables

Variable	Weld no. 1	2	3	4	5	6	7	8	9	10
Moment of inertia, kg · m^2	87.0	87.0	87.0	87.0	87.0	87.0	19.7	35.5	87.0	109.1
Speed of rotation,[a] m/s	8.3	5.8	4.1	5.8	5.8	5.8	5.8	5.8	5.8	5.8
Axial pressure, MPa	22.1	22.1	22.1	7.3	22.1	27.5	22.1	22.1	22.1	22.1
Time to weld, s	11.0	4.9	2.0	5.8	4.9	4.6	2.3	3.6	4.9	6.6
Energy input,[b] J/cm^2	16870	8440	4220	8440	8440	8440	1910	3440	8440	10580

(a) Peripheral velocity.
(b) Total energy input to the weld per unit area.

ness of the machined surfaces was approximately 1.6 μm. In each case the end coupling was clamped in a chuck, rotated to a predetermined speed, and the stationary pipe was brought into contact with the rotating coupling under an applied axial pressure to form the weld. Table 2 lists the welding conditions used in this study to make the test welds.

The finished welds were sectioned along the longitudinal axis, mounted, polished and observed under an optical microscope in the as-welded condition. Some of the welds were studied using a scanning electron microscope (SEM) with an energy-dispersive x-ray fluorescence spectrometer. Notched tensile and impact tests were done on some of the welds after they were quenched and tempered. In these test specimens, the notch was placed along the weld center line to force the break at the weld interface.

Wedges that were 25 × 12 mm (0.98 × 0.47 in.) were cut along the longitudinal axis from the weld area of welds 1 and 2, polished and macroetched. After locating the weld, the wedges were sectioned along the weld center line. The weld interfaces on both steel A and steel B side were then chemically analyzed using a wavelength dispersive x-ray fluorescence spectrometer. This instrument produces x-rays that penetrate up to 0.1 mm (0.04 in.) on the sample surface and, therefore, is considered as an excellent tool for the quantitative chemical analysis of surface layers. Carbon and sulfur contents on the weld interfaces were analyzed using a Leco carbon and sulfur analyzer. Samples from at least two different locations in the weld were extracted for the purpose of chemical analysis.

Results

The Effect of Speed of Rotation

Welds 1 to 3 were made at different speeds of rotation keeping the other two variables, moment of inertia and the axial pressure, constant. As indicated in Table 2, by lowering the speed of rotation the time required to complete the weld dropped from 11 to 2 s. While weld 1 showed concavity at the center, the shape of the weld gradually became convex at the middle—Fig. 1.

Welds which exhibited a bulge outward at the midthickness were described as having convex shape. The welds, which showed an inward bulge towards the weld center line between steel A and steel B at the midthickness (thicker at the outer and inner diameters compared to the midthickness), were described as having concave shape. The amount of flash (the metal pushed out both at the inner and outer diameters) also decreased rapidly with decreasing speed of rotation.

The microstructure consisted of bands of martensite (hardness 624 VHN) and feathery upper bainite (hardness 330 VHN) for weld 1 (Fig. 2), while welds 2 and 3 showed increasing amounts of martensite in the weld area. Steel B side of welds 2 and 3 exhibited scattered bainite in martensite matrix whereas the bainite content in steel A side of the same welds was negligible—Fig. 3.

The Effect of Axial Pressure

The effect of axial pressure on the resultant microstructures was studied using welds 4, 5, and 6. No drastic changes were seen in the time required to complete the weld. Weld 4 was made with the lowest axial pressure and exhibited almost no flash at all. It also exhibited convex shape—Fig. 4A. Several small intergranular cracks were seen both at the outer and inner diameters. Martensite was seen to be the major constituent in the weld area. The steel B side of the weld exhibited scattered areas of bainite in martensite matrix.

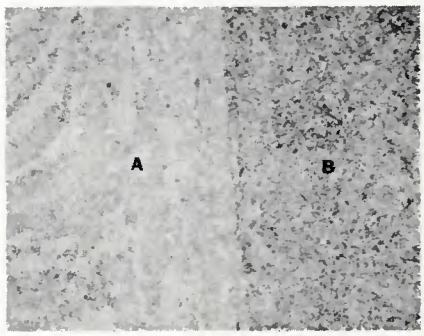

Fig. 2—Weld 1 showing a banded microstructure on steel A side; the white bands showed martensite and the dark bands showed bainite. Picral etch. ×50 (reduced 50% on reproduction)

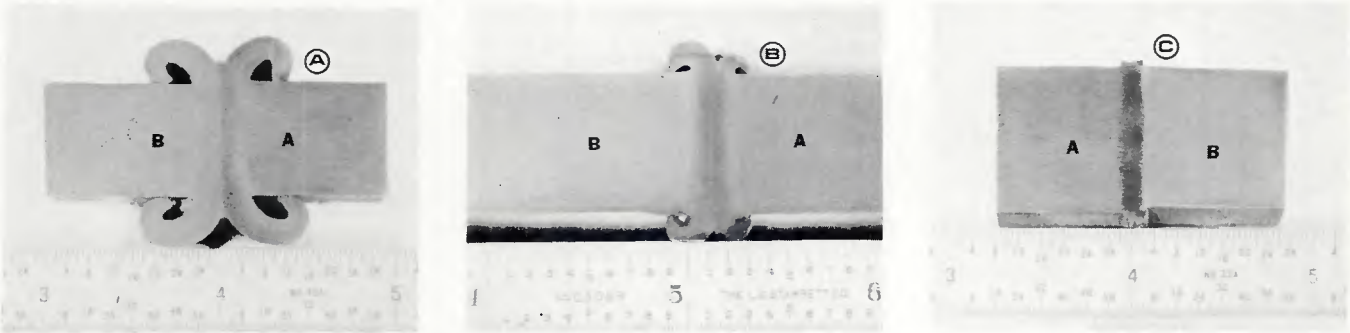

Fig. 1—The effect of speed of rotation (given by the peripheral velocity) on the resultant weld shapes: A—weld 1, 8.3 m/s; B—weld 2, 5.8 m/s; C—weld 3, 4.1 m/s. (A and B in Fig. 1A, B, and C refer to steel A and steel B, respectively) (reduced 50% on reproduction)

Fig. 3 — The microstructure of weld 2. Steel B side showed scattered bainite (dark areas) in martensite matrix. Picral etch. X50 (reduced 50% on reproduction)

Compared to weld 4, welds 5 and 6 exhibited increasingly larger flash. Both welds 5 and 6 exhibited a predominantly martensitic microstructure in the weld area on steel A side. The steel B side of these two welds showed scattered bainite in martensite matrix. The weld shape was concave at the center for welds 5 and 6.

From the interface between the weld and the base metal on steel A side, banding was noticed for weld 6. The bands consisted of alternate layers of martensite and bainite. However, these bands at the edge of the heat-affected zone (interface between the weld and steel A) were only faintly visible in weld 5 and were not as clearly pronounced as in weld 6.

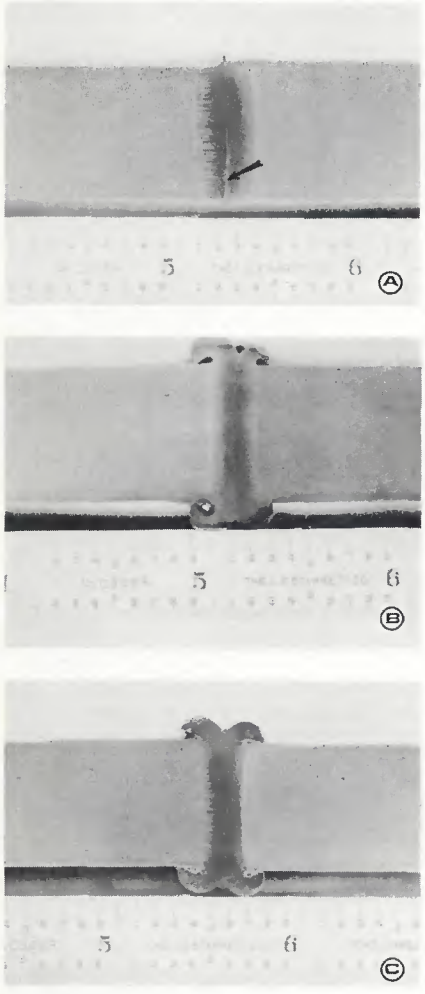

Fig. 4 — The effect of axial pressure on the weld shapes: A — weld 4, 7.3 MPa; B — weld 5, 22.1 MPa; C — weld 6, 27.5 MPa. Note the crack (shown by arrow) in weld 4

The Effect of Moment of Inertia

Welds 7, 8, 9 and 10 were made with increasing moments of inertia, keeping the other parameters constant. As can be seen from Fig. 5A, weld 7 is in two pieces because it was not completely formed. Both welds 7 and 8 showed convex shape, whereas welds 9 and 10 were concave at the center. The time required to weld increased from 2.3 s for weld 7 to 6.6 s for weld 10.

The microstructure in weld 7 consisted of martensite. This weld also exhibited small intergranular cracks. The end regions near the inner and outer diameters of the steel B side of the weld remained unaffected by the heat generated during the welding — Fig. 5A. The weld also exhibited several inclusions near the mating faces. The width of the zone affected by the frictional heat was only 2.48 mm (0.098 in.) — Fig. 6.

Weld 8 exhibited two separate unconnected cracks that originated independently from the outer and inner diameters. Both the cracks were intergranular in nature. The crack that originated at the outer diameter was about 0.2 mm (0.008 in.) from the weld center line. The microstructure in this weld also consisted of martensite.

Fig.6 — Steel B side of weld 7 showing oxide inclusions and a crack near the mating face. Picral etch. X100 (reduced 50% on reproduction)

The microstructure in weld 9 was the same as in welds 2 and 5 and exhibited martensite as the major constituent on steel A side and scattered bainite in martensite matrix on steel B side. Weld 10, upon etching, showed alternate dark and white lines indicating banding in the weld. The banding was much more pronounced in weld 10 than was noticed on steel A side of weld 9. As in the earlier cases, the banding was caused by the formation of light etching martensite and dark etching bainite. Weld 10 also showed a larger flash compared to the other three welds. Compared to weld 9, the microstructure in weld 10 showed more bainite in martensite matrix.

SEM and Chemical Analysis

SEM examination of the fracture surfaces of the impact test specimen from

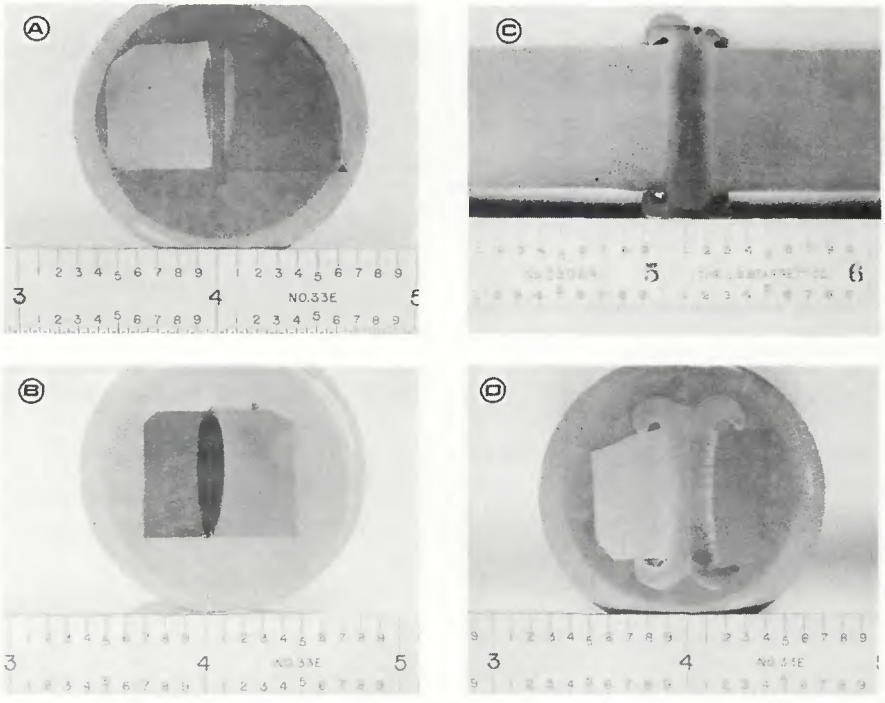

Fig. 5 — The effect of moment of inertia on the weld shapes: A — weld 7, 19.7 kg · m²; B — weld 8, 35.5 kg · m²; C — weld 9, 87.0 kg · m²; D — weld 10, 109.1 kg · m²

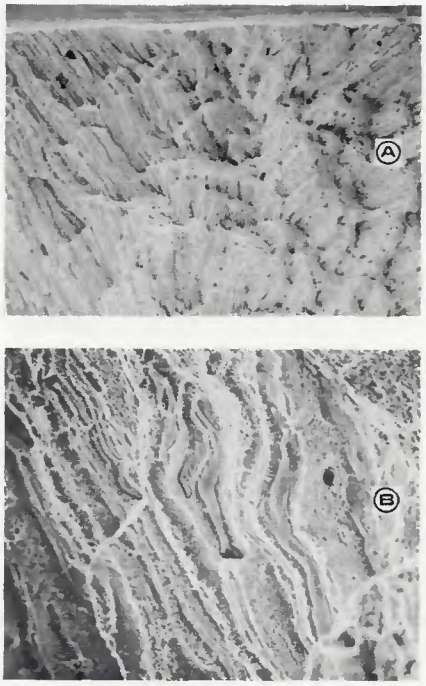

Fig. 7—SEM views of the fracture surfaces on the impact test specimen from weld 1: A—overall view of the fracture surface, X30; B—elongated MnS inclusions near the weld interface oriented perpendicular to the longitudinal axis of the specimens, X500. A and B reduced 50% on reproduction

weld 1 (Fig. 7) revealed that the predominant mode of fracture in the specimen was by microvoid coalescence. The voids and the inclusions appeared to be oriented parallel to the weld interface. Similar reorientation was observed on the fracture surface of the notched tensile specimen. EDS x-ray analysis of the elongated inclusions on the fracture surfaces of both the impact and the tensile specimens indicated that they were of the manganese sulfide type.

The fracture surface of the impact test specimen from weld 2 exhibited no such reorientation of voids or inclusions as observed in weld 1—Fig. 8A. Although the predominant mode of fracture in the impact specimen from weld 2 was by microvoid coalescence, scattered areas of transgranular cleavage were observed—Fig. 8B. Several large voids were observed to be associated with MnS inclusions in all of the specimens.

The results of the chemical analysis conducted on the weld interfaces using a wavelength dispersive x-ray fluorescence spectrometer are presented in Table 3. Weld interfaces on both steel A and steel B sides were analyzed from welds 1 and 2. Comparing the results obtained on steel A side of both the welds with those obtained on unwelded steel A (Table 1), it appears that the chemistry at the weld interfaces remained virtually unchanged. The same conclusion can be drawn comparing the results from steel B side of the weld interfaces with those obtained on unwelded steel B—Table 1.

Discussion

The kinetic energy of a rotating system is given by $\frac{1}{2} I\omega^2$ where I is the moment of inertia of the system and ω its angular velocity. Substituting revolutions per minute (rpm) for angular velocity ω and WK^2 for I of the flywheel system, the kinetic energy of rotation can be given by $(1/5873)\,(WK^2)\,(\text{rpm})^2$ in ft-lb.* Hence by changing either the flywheel weights on the welding machine or the speed of rotation of the parts being welded, the total energy input to the weld can be changed.

In welds 1, 2 and 3, the effect of lowering the speed of rotation was to lower the total energy input into the weld; this meant that the amount of heat generated at the weld interface was lowered. The lowering of the heat input to the weld in low alloy steels resulted in faster cooling of the weld through the lower transformation temperatures (Ref. 1). This explains the reason for the formation of larger amounts of martensite in weld 3 compared to welds 2 and 1.

The size of the flash and the amount of upset in welds 2 and 3 indicate that the extent of plastic working of the metal decreases as the energy input to the weld is decreased. This decrease in the extent of plastic working is also shown by the absence of flow lines in weld 3. The flow lines resulting in a banded microstructure are characteristically seen in forged products.

The absence of flow lines in weld 3 suggests that the frictional heat generated at the weld interface was probably dissipated too soon before any appreciable forging action occurred in the weld. The brittle martensitic microstructure stemming from low energy input to the weld and the lack of any appreciable forging action during welding probably resulted in a poor weld in the case of weld 3.

Studying the inertia welding of low carbon steel solid bars, Lebedev *et al.* (Ref. 11) observed that the heat generated during welding is concentrated at the periphery at low speeds of rotation; also, as the speed of rotation is increased, the zone of most intensive heat generation is displaced to the axis of the specimen. Contrary to this observation, the present results obtained on tubular goods indicate that, as the speed of rotation is decreased, the weld tends to be convex shaped; this suggests that more heat was generated at the center of the specimens rather than at the periphery.

The difference between the current observations and those made by Lebedev *et al.* (Ref. 11) may be explained in terms of differing specimen geometries. In the case of solid bars as the speed of rotation is increased, the relative motion of the parts even near the center increases, generating more heat. However, some of the heat generated at the periphery is probably conducted into the center due to the high thermal gradient that exists between the periphery and the axis of the specimen. Since the total welding time increases with increased speed of rotation, more time will be available for the heat to conduct from the periphery to the axis of the specimen. Much of the heat generated at the center cannot escape to the periphery and remains concentrated there making the weld convex.

In the case of tubular goods used in the study reported here, the difference in the relative motion of parts between the inner and outer diameters is not big; therefore, the thermal gradient is not expected to be much. The fast cooling rates associated with low speeds of rotation appear to cause loss of heat at the periphery to the surrounding. The heat losses at the periphery may be facilitated at low speeds of rotation by the pres-

Wk^2 is the moment of inertia where W is the weight of the flywheel system and k is the radius of gyration; the 5873 is a constant that was mathematically derived from actual operating values (Ref. 10).

Table 3—Results of the Chemical Analysis Conducted at the Weld Interface, %

	Weld 1		Weld 2	
Element	Steel A side	Steel B side	Steel A side	Steel B side
C	0.39	0.43	0.39	0.42
Mn	0.83	1.72	0.83	1.45
Si	0.27	0.22	0.24	0.03
Ni	0.15	<0.005	0.13	<0.005
Mo	0.20	0.15	0.20	0.16
Cu	0.15	0.02	0.11	0.02
Cr	0.89	0.03	0.89	0.04
S	0.014	0.011	0.010	0.008
P	0.015	0.010	0.009	0.013

ence of a small flash. This would make the weld assume a convex shape. As the speed of rotation is increased, the amount of flash formed at the periphery increases. The large flash formed at higher speeds of rotation appears to reduce the radiation heat losses from the periphery, thereby promoting the heat conduction along the longitudinal axis of the pipes; all of this makes the weld assume a concave shape.

Varying the axial pressure does not change the energy input into the weld. Welds 4, 5, and 6 were made with increasing pressure, while the total energy input to the weld was maintained constant. Note that, unlike the case with welds 1, 2, and 3, the time required to complete the weld in the case of welds 4, 5, and 6 showed only a small change.

The measurement of upset of the pieces revealed that increasing the pressure increases the weld upsets also. This is understandable since an increase in the weld pressure in the axial direction would squeeze more metal through the flash, thereby increasing the upset. Since welds 4, 5, and 6 were made with identical energy inputs, weld 6 was subjected to the maximum deformation compared to welds 4 and 5, because it was made with the highest axial pressure. Therefore, the effects of hot working were clearly seen in weld 6 compared to welds 4 and 5. These effects were pronounced banding in the weld, larger flash and upset compared to the other two welds.

One conclusion that may be drawn from welds 4, 5, and 6 is that the major microstructural constituent in all of them is martensite. This suggests that the axial pressure does not have any significant effect on the weld microstructure. This also means that the weld cooling rates in the transformation temperature range are basically dictated by the speed of rotation and the moment of inertia of the flywheel system.

Both the above observations indicate that there is a range of welding variables over which essentially the same microstructure can be produced. In welds 4, 5, and 6, the steel B side of the weld exhibited scattered bainite in martensite matrix. This was to be expected since the hardenabilities of steels A and B are different owing to their compositional differences; therefore, steel B tends to form more bainite than martensite under the present conditions due to its shallow hardenability.

In all of the welds, it was noticed that the amount of flash was much higher on steel B compared to steel A. This difference in the sizes of the flash was especially evident for welds 1, 2, and 10 which were made with relatively higher energy inputs compared to the other welds. During the preparation of the test welds, the inertia welding machine was programmed in such a way that, after the end coupling reached the predetermined speed, the stationary pipe was brought into contact with the rotating coupling under a contact pressure of 1.3 MPa (188.5 psi). When the speed of rotation (peripheral velocity) of the end coupling dropped by 0.42 m/s (99 ipm), the preset axial pressure was applied to form the weld.

A series of temperature measurements made using thermocouples as a function of time at mid-wall thickness of the pipes 1 mm (0.04 in.) from the mating faces indicated that the temperature reached 135°C (275°F) 1 s after the contact occurred between the two parts under a contact pressure of 1.32 MPa (191 psi). Since the drop of 0.42 m/s (99 ipm) in the peripheral velocity of the rotating part occurred in much less than 1 s, it is estimated (based on the temperature measurements made) that the temperature of the mating faces when the axial pressure was applied was probably no more than 400°C (752°F).

In other words, the upsetting of the parts began when they were relatively cold. However, as the upsetting continued, the temperature at the weld interface reached the forging temperature range of the steels. Therefore, the extent to which steel A and steel B were upset depended on their room temperature hardness as well as high temperature strength. Since steel A had higher molybdenum and chromium contents than steel B, it had a better high temperature strength (Ref. 12). The hardnesses of steel A and steel B were 33 HRC and 20 HRC, respectively. Therefore, during the welding of the pipes when the axial pressure was applied, more of steel B would be squeezed out through the flash owing to its lower strength compared to steel A. This may also mean that steel B might have more upset compared to steel A.

The appearance of the flash tended to be more spiral and curly on steel B, while it was more flat and parallel to the longitudinal axis of the parts on steel A. This was probably due to the centrifugal force of the rotating part (steel A) which tended to force the hot, plastic metal along the tangential direction. However, since the material was flowing outward all along the circumference, the centrifugal force would tend to push the squeezed out metal along the longitudinal axis of the parts.

The volumes of the flash on weld 1 measured both at the outer and inner diameters were practically equal. However, the inner diameter flash is thicker (Fig. 1) than that on the outer diameter, because it flowed on a smaller diameter. For weld 2, unlike in weld 1, the volume of the flash at the inner diameter was slightly more than that at the outer diameter. The measurement of the flash volumes also indicated that the total volume of flash generated in weld 1 was almost five times more than that generated on weld 2.

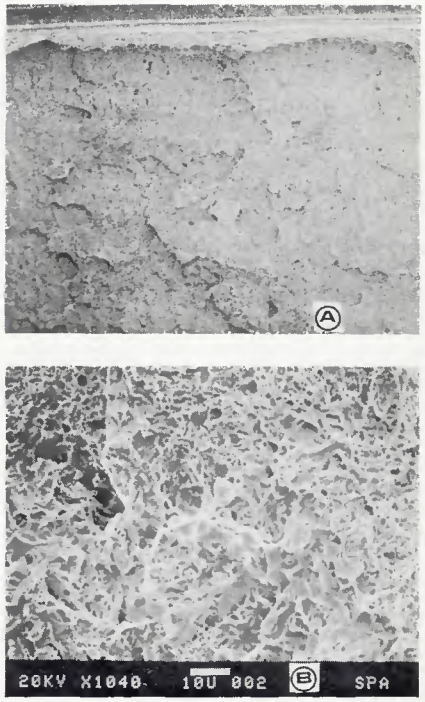

Fig. 8 — SEM views of the fracture surfaces on the impact test specimens from weld 2: A — ×20; B — ×1040. A and B reduced 50% on reproduction

In the case of welds 7 and 8, the energy input was too low to create a bond. The presence of oxide scale on the weld mating faces (Fig. 6) and the presence of oxide inclusions in weld 7 suggest that, even though some frictional heat was generated at the mating faces, it was dissipated too soon for any appreciable forging action to occur. The absence of flow lines in the weld also indicates that practically no forging action occurred in welds 7 and 8. The intergranular cracks seen in weld 8 at the outer and inner diameters could have formed due to a weak bond and a brittle martensitic microstructure in the weld.

The selection of moment of inertia is limited by the availability of the flywheel weights. As the moment of inertia is increased from 19.7 $kg\text{-}m^2$ to 109.1 $kg\text{-}m^2$, the time of welding increased noticeably from 2.3 to 6.6 s. Since the moment of inertia controls the energy input to the weld along with the speed of rotation, a change in the moment of inertia of the system also changes the energy input to the weld. Increasing the energy input to the weld as in welds 9 and 10 caused the formation of more bainite in the weld area suggesting that the weld cooling rates were slower than in welds 7 and 8.

The extent of banding also increased progressively with increasing moment of inertia, indicating that appreciable forging action in the weld caused segregation of the alloying elements along the flow lines. As a result of this segregation, the weld cooling rates transformed the segregated areas differently, leading to a banded microstructure consisting of martensite and bainite. The forging action also caused the grains and the sulfide inclusions to be oriented along the direction of plastic flow of the metal at the weld face, *i.e.,* parallel to the weld center line.

The disadvantage of such a reorientation of the grains parallel to the weld line appears to be the loss of toughness in the weld. The Izod impact energy values at room temperature for weld 1 in the quenched-and-tempered condition were in the vicinity of only 25 J. SEM examination of the fracture surfaces of the impact specimen in Fig. 7 clearly shows the reorientation of the inclusions and the grains that resulted from the forging action during the welding process. The reorientation of the grains and the inclusion along the weld center line suggest that, when the inertia welds are tested in the so-called longitudinal direction of the base materials (with reference to the metal working direction), it is actually the transverse properties of the weld that are exposed to the testing.

The extent of banding in weld 2 was observed to be negligible compared to weld 1, indicating that the amount of plastic working in weld 2 was not substantial. This fact is also confirmed by the absence of reorientation of the sulfide inclusions and the grains in the fracture surface of the impact specimen from weld 2 — Fig. 8. The absence of reorientation of grains and the inclusions in the direction of plastic flow of the metal in weld 2 suggests that a certain minimum energy input to the weld is required to cause the reorientation of the grains and the inclusions at the weld interface.

The chemical analysis using the wavelength dispersive X-ray fluorescence spectrometer conducted approximately 0.75 mm (0.03 in.) from the weld interfaces indicated that, except for noticeable differences in manganese and silicon contents on steel B side of weld 2, the amounts of the other elements remained virtually unaltered when compared to the compositions of the base materials. This suggests that whatever mechanical mixing that may have occurred in the weld (Ref. 13) must have probably occurred within 0.75 mm (0.03 in.) from the weld interface and that no gross compositional changes occurred in the weld.

Conclusion

Based on the study described here the following conclusions may be drawn:

1. The weld microstructures in the inertia friction welding of low alloy steels are essentially controlled by the speed of rotation and the moment of inertia of the flywheel system, both of which control the energy input to the weld. As the energy input to the weld was lowered, the amount of martensite formed in the weld increased and the weld also became convex.

2. Increasing either the speed of rotation or the moment of inertia of the system produced more banding in the material, indicating increased forging action at the weld interface.

3. The axial pressure did not have any significant effect on the weld microstructures; this means that there is a range of welding variables over which essentially the same microstructure can be produced.

4. The inertia friction welds tested had poor impact properties compared to the base materials, probably due to the reorientation of the inclusions at the weld interface.

5. No gross changes in the chemical composition were detected near the weld interfaces compared to the base materials.

Acknowledgments

The author wishes to thank Dr. A. Goldman of Spang and Company for his help with the chemical analysis of the welds and helpful comments on the manuscript. Thanks are also due to Mr. F. J. Stodolsky of this laboratory for his help in preparing the test welds and to the management of Spang and Company for their permission to publish this paper.

References

1. American Society for Metals. 1977. *Metals Handbook* 6 (8): 507, 204. Metals Park, Ohio.

2. Wang, K. K., and Nagappan, P. 1970. Transient temperature distribution in inertia welding. *Welding Journal* 49 (9): 419-s to 426-s.

3. Wang, K. K., and Rasmussen, G. 1972. Optimization of inertia welding process by response surface methodology. *Trans. ASME, Journal of Energy for Industry* 94 (4): 999-1006.

4. Wang, K. K., and Lin, W. Flywheel friction welding research. *Welding Journal* 53(6): 233-s to 241-s.

5. Novikova, L. N. 1978. The effect of the moment of inertia of flywheel mass on the structure and properties of welds in steel 45 made by inertia welding. *Svar. Proiz* 11: 41-42.

6. Novikova, L. N., *et al.* 1977. The properties of joints made by inertia welding. *Svar. Proiz* 8: 31-32.

7. Eberhart, T. N. and Quenney, R. A. 1977. Inertia (friction) welding of P/M parts. *International Journal of Powder Metallurgy and Powder Technology* 12 (4): 273-275, 277-278.

8. Hallet, W. M. 1976. *A review of inertia welding.* SME Technical Paper AD76-909. Dearborn, Michigan: Society of Manufacturing Engineers.

9. Baxter, D. F. 1976. Problem solving with inertia welding. *Metal Progress* 110 (2): 37-41.

10. American Welding Society. 1980. *Welding handbook,* ed. W. H. Kearns, 7th ed., vol. 3, p. 251. Miami, Florida.

11. Lebedev, V. K., *et al.* 1980. The inertia welding of low-carbon steel. *Avt. Svarka* 7: 18-22.

12. Bain, E. C., and Paxton, H. W. 1966. *Alloying elements in steel.* Metals Park, Ohio: American Society for Metals.

13. Wang, K. K. April 1975. *Friction welding.* WRC bulletin 204. New York, N.Y.: Welding Research Council.